

## Electron States in a Lattice of Au Nanoparticles: The Role of Strain and Functionalization

Ronaldo J. C. Batista,<sup>1</sup> Mário S. C. Mazzoni,<sup>1</sup> Ignacio L. Garzón,<sup>2</sup> Marcela R. Beltrán,<sup>3</sup> and Helio Chacham<sup>1,\*</sup>

<sup>1</sup>*Departamento de Física, ICEX, Universidade Federal de Minas Gerais, CP 702, 30123-970, Belo Horizonte, MG, Brazil*

<sup>2</sup>*Instituto de Física, Universidad Nacional Autónoma de México, Apartado Postal 20-364, Mexico, D.F., 01000 Mexico*

<sup>3</sup>*Instituto de Investigaciones en Materiales, Universidad Nacional Autónoma de México,*

*Apartado Postal 70-360, Mexico, D.F., 04510 Mexico*

(Received 25 October 2005; published 23 March 2006)

We make use of first-principles calculations to study the effects of functionalization and compression on the electronic properties of 2D lattices of Au nanoparticles. We consider Au<sub>38</sub> particles capped by methylthiol molecules and possibly functionalized by the dithiolated conjugated molecules benzenedimethanethiol and benzenedicarbothialdehyde. We find that the nonfunctionalized lattices are insulating, with negligible band dispersions even for a compression of 20% of the lattice constant. Distinct behaviors of the dispersion of the lowest conduction band as a function of compression are predicted for functionalized lattices: The band dispersion of the benzenedimethanethiol-functionalized lattice increases considerably with compression, while that of the benzenedicarbothialdehyde-functionalized lattice decreases.

DOI: [10.1103/PhysRevLett.96.116802](https://doi.org/10.1103/PhysRevLett.96.116802)

PACS numbers: 73.21.-b, 73.22.-f, 73.63.Rt

Gold and silver particles with diameters from one to a few nanometers can be produced by limiting particle nucleation with a protective cap of organic molecules [1]. If the metal cores have similar diameters, these nanoparticles can self-assemble into nearly crystalline two-dimensional lattices [2]. One-dimensional [3] and three-dimensional [4] lattices of Au nanoparticles can be produced as well.

The arrangement and the physical properties of lattices of metal nanoparticles are dependent on the metal core characteristics (such as size and composition), as well as on the protective agents [5] and on mechanical compression [6]. Electronic properties of such lattices have been experimentally investigated by several techniques. X-ray absorption and photoemission experiments [7] indicate a vanishing density of electronic states at the Fermi energy  $E_F$  for very small alkanethiolate-capped Au particles (with diameter  $\sim 1.6$  nm), consistent with a nonmetallic behavior. Scanning microscope experiments [6,8] indicate that lattices of alkanethiolate-capped Au particles are insulators and that mechanical compression may induce a insulator-to-metal transition. However, electron transport measurements failed to observe true metallic (nonthermally activated) conduction on compressed lattices [9].

The protective agents of the nanoparticles, as well as further functionalization by organic molecules, can also be used to modify the electron and spin transport between nanoparticles in a lattice or an array. Recently, Dadosh *et al.* [10] investigated the electrical conduction through isolated pairs of Au nanoparticles connected by benzenedimethanethiol (BDMT) and other dithiolated conjugated molecules. BDMT molecules have also been used as molecular bridges [11] to mediate spin transfer between CdSe nanoparticles. In the present work, we make use of first-principles calculations to study the effects of functionalization and compression on the electronic properties of two-

dimensional lattices of Au nanoparticles. We consider Au<sub>38</sub> nanoparticles capped by methylthiol molecules and possibly connected by BDMT and benzenedicarbothialdehyde (BDCT). The structures of BDCT and BDMT are schematically shown in Fig. 1. Our methodology is based on the density functional theory [12] within the generalized gradient approximation [13] and norm-conserving pseudopotentials [14] as implemented in the SIESTA [15,16] code. The solutions of the Kohn-Sham equations are expanded as a linear combination of atomic pseudowave functions of finite range. We use a basis set that was previously used to study methylthiol-capped Au nanoparticles [17].

As a model to describe the Au nanoparticle lattices, we consider a single-layer, infinite 2D crystal of Au<sub>38</sub> nanoparticles with one nanoparticle per unit cell. The nanoparticle is capped by methylthiol molecules and its geometry is fully optimized [18]. In the optimized geometry, the sulfur atom of each methylthiol molecule binds to two Au atoms at the nanoparticle surface with bond lengths between 0.24 and 0.26 nm. The initial geometry of the 2D crystal was that of a triangular lattice, consistent with the experimental observations. We also consider possible functionalizations of the capped Au<sub>38</sub> particle where four methylthiol molecules are replaced by two BDMT or BDCT molecules that connect neighboring particles [19]. The in-plane lattice vectors and the atomic coordinates of the resulting 2D crystals are optimized at zero pressure. In the perpendicular direction, the unit cell is large enough to

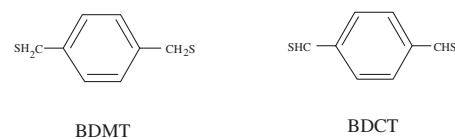


FIG. 1. Schematic structures of BDMT and BDCT.

avoid interactions between successive periodic images. Such a model for an isolated (unsupported) 2D crystal would simulate situations where the layer is not deposited on a strongly interacting substrate that could modify its electronic structure. Similarly to the methylthiol case, the sulfur atom at each end of BDMT and BDCT binds to two Au atoms at the nanoparticle surface, with bond lengths in the 0.24–0.25 nm range for BDMT and in the 0.24–0.26 nm range for BDCT. Figure 2 shows the unit cell and first neighbors of a lattice of  $\text{Au}_{38}$  nanoparticles connected by BDCT. The lattice of nonconnected (i.e., only methylthiol-covered) particles and that of the BDMT-connected particles are similar to that in Fig. 2.

The band structure of the 2D crystal of methylthiol-capped Au nanoparticles without compression is shown in Fig. 3(a). The figure depicts the highest valence band and the two lowest conduction bands, all of them with negligible dispersions. In the absence of compression, the equilibrium distance between the protective agents of neighboring nanoparticles is approximately 0.4 nm, which indicates that the interaction between nanoparticles is very weak. The corresponding equilibrium distance between the closest Au atoms of neighboring nanoparticles is 0.84 nm. These large distances result in negligible electron hopping matrix elements between particles as indicated by the dispersionless bands. The calculated electronic structure is that of a semiconductor with a density functional theory (generalized gradient approximation) gap of 0.22 eV, which is consistent with the nonmetallic behavior of small Au particles observed by Zhang and Sham [7]. In typical experimental situations, the alkanethiol molecules used to cap the Au particles are longer than the methylthiol molecules considered here. Consequently, the equilibrium distance  $d_{ss}$  between the surface Au atoms of neighboring particles in uncompressed lattices is larger in typical experimental situations ( $d_{ss} > 2$  nm) [6] than in our model ( $d_{ss} = 0.84$  nm). Therefore, the (negligible) electron coupling between neighboring methylthiol-covered particles

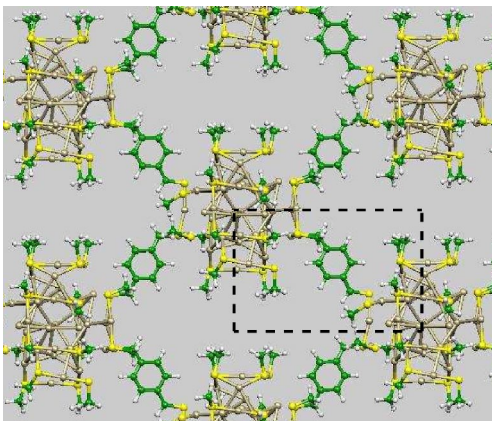


FIG. 2 (color online). Lattice of methylthiol-capped  $\text{Au}_{38}$  nanoparticles connected by BDCT.

calculated in the present work can be considered as an upper bound to the corresponding coupling for uncompressed lattices of particles covered by longer alkanethiol molecules. This is consistent with the absence of electronic conduction in uncompressed lattices of alkanethiol-covered Au particles [5].

The results described so far indicate that uncompressed lattices of alkanethiol-covered Au particles should be insulating. We now turn to possible nanoparticle functionalizations that might lead to conducting behaviors. We will consider nanoparticles connected by BDCT or BDMT molecules. BDMT molecules have been successfully used as molecular bridges between Au nanoparticles [10] and between CdSe nanoparticles [11]. The optimized geometry of the lattice functionalized by BDCT is shown in Fig. 2. The lattice functionalized by BDMT is very similar.

Figure 3(b) shows the energy bands of the lattice functionalized by BDMT without compression, near the Fermi energy. As it is possible to see, the band gap does not change significantly as compared to the one of the non-functionalized lattice already shown in Fig. 3(a), and the dispersion of the bands is still negligible in the energy scale of the figure. Therefore, functionalization by BDMT does not induce significant electron hopping between particles in the uncompressed lattice. This is consistent with the small conductance of Au-BDMT-Au molecular junctions,

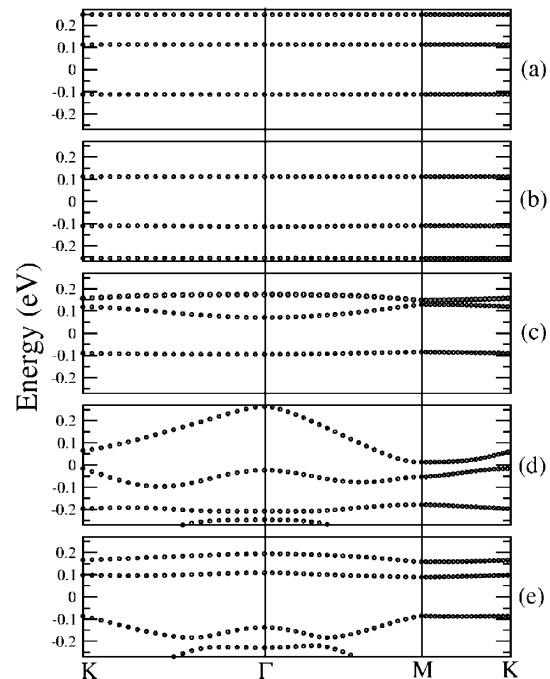


FIG. 3. Energy bands of lattices of methylthiol-covered Au nanoparticles on several situations: (a) without connecting molecules, without compression; (b) connected by BDMT, without compression; (c) connected by BDMT, lattice parameter reduced by 10%; (d) connected by BDCT, without compression; (e) connected by BDCT, lattice parameter reduced by 10%. The Fermi energy is set to zero.

of the order of  $0.0006G_0$  [20], where  $G_0 = 2e^2/h$  is the conductance quantum. The small value of the hopping matrix elements originates from the  $sp^3$  hybridization of the carbon atoms neighbors to the sulfur atoms in BDCT, which prevents the coupling between the  $\pi$  orbitals of the central C6 ring with the nanoparticle surface states. In contrast, in BDCT the carbon atoms connected to the sulfur atoms are trivalent and in the  $sp^2$  hybridization, allowing for a “bridge” of  $\pi$  orbitals between nanoparticles. Such a  $\pi$  bridge is clearly seen in Fig. 4(b), where we show the electron density corresponding to the lowest unoccupied band. As a consequence of the  $\pi$  bridge, the energy bands of the uncompressed lattice of BDCT-functionalized particles show a considerable dispersion, as shown in Fig. 3(d). Although the band structure is still that of a semiconductor, the dispersion of both the uppermost valence band and the lowest conduction band would allow conduction for electron- or hole-doped lattices.

Changes in the transport properties of the 2D lattices of Au nanoparticles due a plane stress could make viable their further use as electromechanical devices. In order to simulate a two-dimensional compression, the prismatic unit cell was submitted to a homogeneous strain in the plane of the array. The lattice parameter was reduced by 10% (approximately 0.2 nm) in the lattices functionalized by BDCT and BDMT and at most by 20% in the nonfunctionalized lattice. After the reduction, the unit cell vectors were fixed and then the geometry of the functionalized Au nanoparticles was allowed to relax. In the case of a superlattice functionalized with BDCT molecules, the calculated force

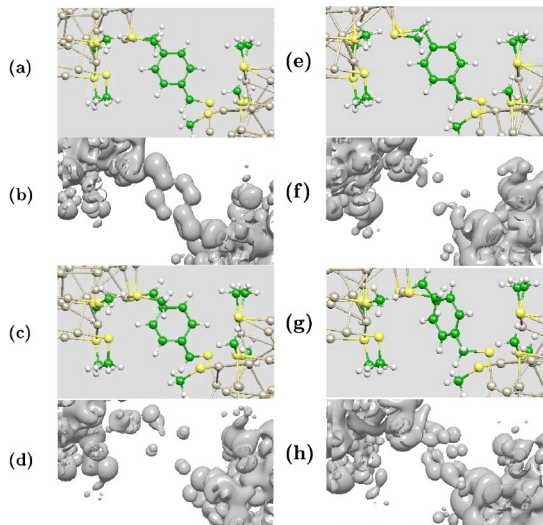


FIG. 4 (color online). (a) Enlargement of the indicated region in Fig. 2, showing the BDCT molecule connecting two neighbors nanoparticles. (b) Electron density corresponding to the lowest unoccupied band of the uncompressed superlattice functionalized with BDCT shown in Fig. 3(d). (c),(d): Same as (a),(b) but for a lattice compressed by 10%. (e)–(h): Same as (a)–(d) but for a lattice functionalized with BDMT and showing the region near a BDMT molecule.

per unit of length required to reduce the unit cell length by 10% was 1.56 N/m.

Figure 3(c) shows the band structure of the lattice of nanoparticles connected by BDCT with a lattice parameter reduction of 10%. A comparison between this figure and Fig. 3(b) shows that the dispersion of the lowest conduction band increases (to 0.06 eV) and the band gap decreases from 0.22 to 0.15 eV as a result of the compression. In a lattice of unconnected particles (covered only with methylthiol molecules), with the same lattice parameter reduction, the dispersion of the conduction band increases only to 0.005 eV. Even a 20% compression of the unconnected lattice is not able to produce a band dispersion larger than 0.007 eV. Therefore, the increase in the conduction band dispersion of the BDCT-connected lattice upon compression is associated with the connecting BDCT molecules and not to the overlap between neighboring nanoparticles surface states. This can also be seen in Figs. 4(e)–4(h), which show that the lowest conduction band becomes delocalized upon compression through a bridge of BDCT  $\pi$  orbitals.

A very different effect occurs when a lattice of Au nanoparticles connected by BDCT is submitted to a two-dimensional compression. The band structure of the compressed lattice is shown in Fig. 3(e). In this case, the dispersion of the lowest conduction band decreases from 0.25 to 0.02 eV and the band gap increases from 0.03 to 0.17 eV. Figure 4 shows that the reduction of the conduction band dispersion is associated with the localization of the conduction band states at the nanoparticles. In order to investigate possible reasons for this effect, we performed calculations for the isolated BDCT with the same geometry as in the uncompressed and compressed lattices, as well as for the system comprised of the BDCT and the three closest Au atoms on each side. In the case of the isolated BDCT, we find that, although the molecule is bent, no important changes occur on low-lying unoccupied states. In contrast, in the case of the  $3\text{Au} + \text{BDCT} + 3\text{Au}$  system, the lowest unoccupied orbital becomes more localized on the  $3\text{Au-S}$  bond regions and less localized on the C6 ring, similar to what is observed in Figs. 4(a)–4(d). Therefore, the changes in conduction band wave function seem to be related to the local binding between the sulfur atom and the neighboring Au atoms in the nanoparticles and not to changes in the BDCT geometry.

The band structures shown in Fig. 3 were calculated using a LCAO-*ab initio* (the SIESTA [15,16]) method, which takes into account the manifold of all the valence bands and more than 3 times as many conduction bands. In the following, we will show that the dispersion of the lowest conduction band can be described by a much simpler single-band model. In this description, we consider each Au nanoparticle as a single site, with only one orbital per site, and a tight-binding Hamiltonian  $H = E_0 - \sum t_{ij}c_i^\dagger c_j$ , where  $t_{ij} = t$  between sites connected by BDCT



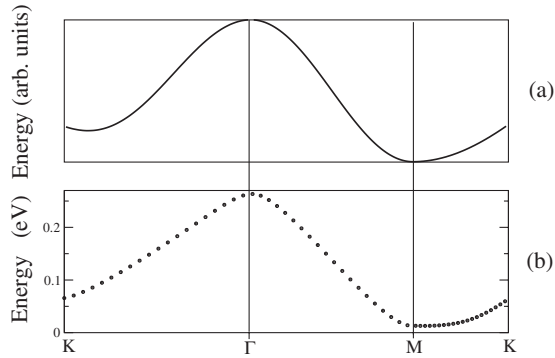


FIG. 5. (a) Band dispersion of a one-band tight-binding Hamiltonian with hopping  $t$  between connected nanoparticles. (b) Upper band of Fig. 3(d).

and zero otherwise. This two-parameter Hamiltonian fits very well (with  $t = -0.031$  eV) the lowest conduction band of the uncompressed lattice of BDCT-connected particles, as shown in Fig. 5. The lowest conduction bands of the compressed BDCT-connected lattice and the compressed BDMT-connected lattice are equally well fitted by the model, with  $t = -0.003$  eV and  $t = 0.008$  eV, respectively. Such a strong dependence of the electron hopping between nanoparticles as a function of compression and functionalization might be observed in transport measurements.

In summary, we performed a first-principles study of electronic and structural properties of 2D lattices of  $\text{Au}_{38}$  nanoparticles capped by methylthiol molecules and possibly functionalized by the dithiolated conjugated molecules BDMT and BDCT. We find that the nonfunctionalized lattices are insulating, with negligible band dispersions even for a compression of 20% of the lattice constant, which reduces the smallest Au-Au distance between particles to 0.47 nm. Distinct behaviors of the dispersion of the lowest conduction band as a function of compression are predicted for functionalized lattices: The conduction band dispersion of the BDMT-functionalized lattice increases considerably with compression, while that of the BDCT-functionalized lattice decreases.

We acknowledge support from the Brazilian agencies CNPq, FAPEMIG, and Instituto do Milênio em Nanociências-MCT, and from the Conacyt-Mexico Projects No. 40393-F and No. 43414-F. We also thank J. F. Sampaio for fruitful discussions.

\*Corresponding author.

Electronic address: chacham@fisica.ufmg.br

- [1] M. Brust, M. Walker, D. Bethell, D.J. Schiffrin, and R. Whyman, *J. Chem. Soc. Chem. Commun.* **1994**, 801 (1994).
- [2] A. Ulman, *Chem. Rev.* **96**, 1533 (1996).
- [3] T. Teranishi, A. Sugawara, T. Shimuzu, and M. Miyake, *J. Am. Chem. Soc.* **124**, 4210 (2002).
- [4] H. Fan *et al.*, *Science* **304**, 567 (2004).
- [5] T. Teranishi, *C.R. Chim.* **6**, 979 (2003).
- [6] P. Liljeroth *et al.*, *J. Am. Chem. Soc.* **126**, 7126 (2004).
- [7] P. Zhang and T.K. Sham, *Phys. Rev. Lett.* **90**, 245502 (2003).
- [8] S.H. Kim *et al.*, *J. Phys. Chem. B* **103**, 10341 (1999).
- [9] J.F. Sampaio, K.C. Beverly, and J.R. Heath, *J. Phys. Chem. B* **105**, 8797 (2001).
- [10] T. Dadoosh *et al.*, *Nature (London)* **436**, 677 (2005).
- [11] M. Ouyang and D.D. Awschalom, *Science* **301**, 1074 (2003).
- [12] W. Kohn and L.J. Sham, *Phys. Rev.* **140**, A1133 (1965).
- [13] J.P. Perdew, K. Burke, and M. Ernzerhof, *Phys. Rev. Lett.* **77**, 3865 (1996).
- [14] N. Troullier and J.L. Martins, *Phys. Rev. B* **43**, 1993 (1991).
- [15] P. Ordejón, E. Artacho, and J.M. Soler, *Phys. Rev. B* **53**, R10441 (1996).
- [16] J.M. Soler, E. Artacho, J.D. Gale, A. Garcia, J. Junquera, P. Ordejón, and D. Sánchez-Portal, *J. Phys. Condens. Matter* **14**, 2745 (2002).
- [17] I.L. Garzón, C. Rovira, K. Michaelian, M.R. Beltran, P. Ordejón, J. Junquera, D. Sánchez-Portal, E. Artacho, and J.M. Soler, *Phys. Rev. Lett.* **85**, 5250 (2000).
- [18] I.L. Garzón, M.R. Beltran, G. González, I. Gutierrez-González, K. Michaelian, J.A. Reyes-Nava, and J.I. Rodríguez-Hernández, *Eur. Phys. J. D* **24**, 105 (2003); I.L. Garzón *et al.*, *Nanotechnology* **12**, 126 (2001).
- [19] To generate the initial geometry of the BDMT-functionalized lattice, we choose the two pairs of methylthiol molecules in nearest-neighbor particles that are the closest to each other and replaced the closest H atoms within each pair by a  $\text{C}_6\text{H}_4$  ring. Therefore, the binding geometry between the S atoms of BDMT and the particle is the same as that of the (optimized) methylthiol molecules. To generate the initial geometry of the BDCT-functionalized lattice, we removed one H atom at each end of the BDMT molecules in the lattice. Other (less stable) binding geometries between the thiol groups and the particles could arise, for instance, from bond stretching, but these effects are not considered in this work.
- [20] X. Xiao, B. Xu, and N.J. Tao, *Nano Lett.* **4**, 267 (2004).